RESEARCH ARTICLE
Cytoskeleton, February 2013 70:74–84 (doi: 10.1002/cm.21091)

Mechanical and Functional Properties of Epothilone-Stabilized Microtubules

Dezhi Yu,[1] Veronica Pessino,[2] Steve Kuei,[3] and Megan T. Valentine[4]*

[1]Department of Materials, University of California, Santa Barbara, California
[2]College of Creative Studies and Department of Physics, University of California, Santa Barbara, California
[3]Research Internships in Science and Engineering, Materials Research Laboratory, University of California, Santa Barbara, California
[4]Department of Mechanical Engineering, University of California, Santa Barbara, California

Received 7 August 2012; Revised 17 October 2012; Accepted 22 October 2012
Monitoring Editor: George Bloom

Using a suite of biophysical tools, we assess the mechanical, structural, and functional properties of microtubules (MTs) stabilized by the chemotherapeutic compounds epothilone-A, epothilone-B, and taxol in vitro. We demonstrate that MTs stabilized by epothilone-A or epothilone-B are competent to bind tau proteins and support kinesin translocation. Kinesin speed is sensitive not only to the type of small molecule stabilizer used but also to the presence of the essential MT-associated protein tau. Epothilone-stabilized MTs are substantially less stiff than taxol-stabilized MTs. The addition of tau proteins to MTs stabilized by either epothilone compound or taxol further reduces stiffness. Taken together, these results suggest that small molecule stabilizers do not simply stabilize a "native" MT structure, but rather they modulate the structure, function, and mechanics of the MTs they bind. This may have important consequences to the therapeutic use of these agents in cancer chemotherapies. © 2012 Wiley Periodicals, Inc

Key Words: motility, kinesin, tau, microtubules, stiffness, chemotherapeutics

Introduction

Taxanes and epothilones are potent chemotherapeutic drugs that target a broad spectrum of solid mass tumors by inhibiting microtubule (MT) dynamics, arresting mitosis, and inducing cell death [Bollag et al., 1995; Cortes and Baselga, 2007; Alvarez et al., 2011]. Although these compounds are effective in reducing tumor size and improving survival rates, they can generate disabling and dose-limiting neuropathic side-effects, including pain and loss of sensation, which limit their clinical use [Hagiwara and Sunada, 2004; Argyriou et al., 2008; Wolf et al., 2008; Lema et al., 2010]. The molecular basis of these effects is poorly understood, and as a result there are no approved therapies for the prevention or mitigation of chemotherapy-induced peripheral neuropathy (CIPN) [Park et al., 2008; Wolf et al., 2008]. Onset of symptoms not only reduces quality of life but also impacts health and survival due to treatment delays and discontinuations. Interestingly, axonal dysfunction has been observed within the first month of treatment, well before the typical onset of pain symptoms [Park et al., 2011]. This raises the possibility that MT-based kinesin transport and/or the MTs themselves may be altered by the stabilizing compounds, and more importantly, suggests that early or prophylactic interventions might be possible, if quantitative, predictive models of the molecular mechanisms of CIPN were known.

Although taxol-stabilized MTs have been used extensively in in vitro measurements of MT stiffness and kinesin-based motility, there have been very few reports of the effects of other anticancer therapeutics [Gittes et al., 1993; Mickey and Howard, 1995; Block et al., 2003; Vershinin et al., 2007; Dixit et al., 2008]. To address this, we use in vitro assays to directly measure the stiffness of, and the rates and patterns of collective kinesin translocation along, MTs that have been assembled by a variety of small molecule stabilizers and coated with the essential MT-associated protein (MAP) tau [Valdman et al., 2012].

Tau is a neural MAP that binds to MTs, promotes tubulin polymerization, regulates MT dynamics, and is essential for the normal development and maintenance of the nervous system [Saxton et al., 1991; Ferreira et al., 1992; Hurd et al., 1996; Ebneth et al., 1998; Tanaka

Additional Supporting Information may be found in the online version of this article.

*Address correspondence to: Megan T. Valentine, Department of Mechanical Engineering, Engineering II Building, Room 2361C, University of California, Santa Barbara, California 93106. E-mail: valentine@engineering.ucsb.edu

Published online 10 December 2012 in Wiley Online Library (wileyonlinelibrary.com).

et al., 1998; Trinczek et al., 1999; LaMonte et al., 2002; Stamer et al., 2002; Mandelkow et al., 2003; Feinstein and Wilson, 2005; Kieran et al., 2005; Stokin et al., 2005]. Through alternative RNA splicing, a single tau gene produces six different tau isoforms, each of which possesses either three or four imperfect repeats in the C-terminal half of the protein ("3R tau" or "4R tau"), separated from one another by shorter inter-repeats [Lee et al., 1988; Himmler et al., 1989; Himmler, 1989]. In addition, each tau isoform possesses either zero, one, or two inserts in the N-terminal portion of the protein [Hirokawa et al., 1988; Himmler et al., 1989; Himmler, 1989; Chen et al., 1992].

In this study, we focus on the "short" tau isoforms with zero N-terminal inserts (referred to simply as "3R" or "4R" herein), which are abundantly expressed in neurons, and have strong MT binding and regulatory activities [Vershinin et al., 2007; Dixit et al., 2008]. We demonstrate that MTs stabilized by epothilone compounds bind tau proteins with affinities that are similar to those of taxol-stabilized MTs. However, we find that epothilone-stabilized MTs are softer than taxol-stabilized MTs, and that they support slower rates of kinesin translocation when cargos are moved in the presence of tau.

Results

Cosedimentation Assays Assess Ability of MTs to Bind Tau

To assess the ability of epothilone-stabilized MTs to bind wild-type tau isoforms, we performed cosedimentation assays in which MTs are assembled in the presence of either epothilone-A or epothilone-B, then coated with tau. We used a total tubulin dimer to tau molar ratio of 5:1 or 30:1, which brackets the approximate physiological range for neurons [Binder et al., 1985; Drubin et al., 1985]. Previous results have demonstrated that tau binds to MTs in the absence of stabilizing agents and to taxol-stabilized MTs with a high affinity in this concentration range [Peck et al., 2011] (Yu D, Pessino V, LaPointe N, Guzman E, Wilson L, Feinstein S, Valentine M, unpublished observations).

We find no obvious differences between the abilities of MTs stabilized with epothilone-A or epothilone-B to bind either tau isoforms, as shown in Fig. 1. To assess the statistical significance of these data, we use a two-sample Student's *t*-test, we find that the ratios of polymerized tubulin dimers to bound tau are indistinguishable under these conditions (full results of statistical tests are available in Table I). Consistent with prior results, we find that the ratio of tubulin in the MT polymer to bound tau is smaller than the ratio of free tubulin to tau in the initial mixture, since not all tubulin dimers are incorporated into the polymer (especially at higher tubulin:tau molar ratios)

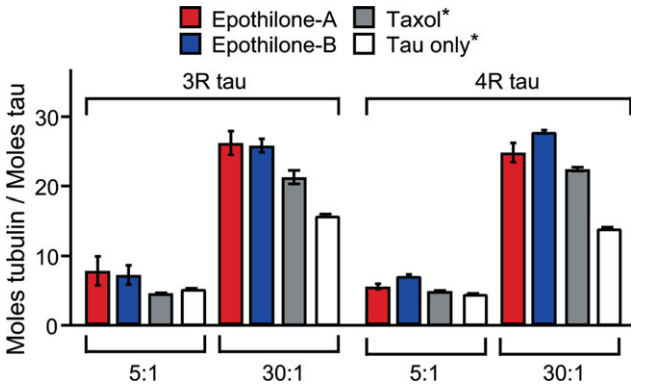

Fig. 1. Results of cosedimentation assay. The ability of tau to bind to epothilone-stabilized MTs was assessed for both epothilone-A and epothilone-B. These data were compared to cosedimentation data obtained with taxol-stabilized and tau-assembled MTs. In each case, two tubulin:tau ratios were tested, 30:1 and 5:1 which span the physiological range in neurons, for both 3R and 4R tau. Full statistical analysis of these data is given in Table I. For each condition, the number of data points $N = 2$ or 3. Error bars are SEM. *Yu, et al., unpublished observations.

and tau binds strongly to MTs but not tubulin subunits [Peck et al., 2011].

We then compared the tau binding behavior of the epothilone-stabilized MTs to that of MTs stabilized with taxol. Qualitatively, we find that MTs stabilized with taxol appear to bind slightly more tau than do MTs stabilized with either epothilone compound, as shown in Fig. 1. Using a two sample Student's *t*-test, we find that the differences between MTs stabilized with epothilone-A and taxol are not significant to the 95% confidence level under any tau condition. For MTs stabilized with epothilone-B, there are significant differences for 4R tau at both the 5:1 and 30:1 tubulin:tau ratio, and for 3R tau at the 30:1 tubulin:tau ratio. For both the taxol- and epothilone-stabilized MTs, we find a reduction in the amount of bound tau as compared to MTs that have been polymerized in the presence of tau but without small-molecule stabilizers. This reduction is significant for all taxol-stabilized MTs, and for all epothilone-stabilized MTs at the 30:1 tubulin:-tau ratio. At the 5:1 tubulin:tau ratio, only the 4R binding to epothilone-B-stabilized MTs was statistically different from the binding of 4R to MTs in the absence of small molecule drugs. This suggests that in the absence of stabilizers, MTs adopt different conformations that modulate the tau binding affinity, or that some fraction of the tau proteins are incorporated on the inner surface of the MT that is not easily accessible after polymerization, or both.

At the 30:1 tubulin:tau ratios, less tau is present in the initial mixture, and it is likely that differences in the amount of bound tau arise from actual differences in binding affinity since there is ample space on the MT for tau to bind. By contrast, at the 5:1 tubulin:tau ratio,

Table I. Results of Statistical Analysis of Cosedimentation Data

Condition 1	Condition 2	*h*	*P*-value
EpA 3RS 5:1	EpA 4RS 5:1	0	
EpA 3RS 30:1	EpA 4RS 30:1	0	
EpB 3RS 5:1	EpB 4RS 5:1	0	
EpB 3RS 30:1	EpB 4RS 30:1	0	
EpA 3R 5:1	EpB 3R 5:1	0	
EpA 4R 5:1	EpB 4R 5:1	0	
EpA 3R 30:1	EpB 3R 30:1	0	
EpA 4R 30:1	EpB 4R 30:1	0	
EpA 3R 5:1	TX 3R 5:1	0	
EpA 4R 5:1	TX 4R 5:1	0	
EpA 3R 30:1	TX 3R 30:1	0	
EpA 4R 30:1	TX 4R 30:1	0	
EpB 3R 5:1	TX 3R 5:1	0	
EpB 4R 5:1	TX 4R 5:1	1	$P<0.01$
EpB 3R 30:1	TX 3R 30:1	1	$P<0.05$
EpB 4R 30:1	TX 4R 30:1	1	$P<0.05$
EpA 3R 5:1	3R 5:1	0	
EpA 4R 5:1	4R 5:1	0	
EpA 3R 30:1	**3R 30:1**	**1**	***P*<0.01**
EpA 4R 30:1	**4R 30:1**	**1**	***P*<0.01**
EpB 3R 5:1	3R 5:1	0	
EpB 4R 5:1	**4R 5:1**	**1**	***P*<0.001**
EpB 3R 30:1	**3R 30:1**	**1**	***P*<0.001**
EpB 4R 30:1	**4R 30:1**	**1**	***P*<0.001**
TX3 R5:1	**3R 5:1**	**1**	***P*<0.001**
TX4 R5:1	**4R 5:1**	**1**	***P*<0.05**
TX 3R 30:1	**3R 30:1**	**1**	***P*<0.001**
TX 4R 30:1	**4R 30:1**	**1**	***P*<0.01**

A two-sample Student's *t*-test (implemented in MATLAB) is used to compare the cosedimentation data to identify statistically significant differences in tau binding. An h value of 1 indicates a significant difference at a minimum confidence level of 95%. P value ranges are shown for data where $h = 1$. The labels at each condition give the type of small molecule stabilizer used (EpA = Epothilone-A, EpB = Epothilone-B, TX = taxol), the type of tau protein used (3R or 4R), and the molar ratio of tau:tubulin dimer in the original mixture.

packing considerations on the MT surface become more important. In this limit of high tau concentration, we find fewer differences between the various polymerization conditions, suggesting that filament geometry begins to dominate in this regime.

Effects of Small-Molecule Stabilizers and Tau on MT Stiffness

We next assessed the mechanical properties of epothilone-stabilized MTs using a spectral analysis method that allows the stiffness of a freely diffusing filament to be determined from the ensemble of shapes it adopts under thermal excitation [Gittes et al., 1993]. In this approach, movies of fluctuating rhodamine-labeled MTs are collected, and the MT shape is fit in each frame to a continuous curve described by a series of Chebyshev polynomials [Valdman et al., 2012]. The variance of the mode amplitudes is then compared to predictions made by the worm-like chain (WLC) polymer model to determine the persistence length, L_p, a common measure of biopolymer stiffness. Physically, L_p is the length over which the filament tangent angle becomes decorrelated. L_p depends both on filament shape and intrinsic materials properties: $L_p = EI/k_BT$ where EI is the flexural rigidity and k_BT is the thermal energy. For isotropic homogeneous structures, EI is the product of the Young's modulus E and the geometric moment of inertia I. Although deviations from WLC behavior have been observed for short MTs (<7 μm), the MTs used in our study range from 10 to 20 μm, significantly longer than this cutoff [Taute et al., 2008].

Consistent with prior studies, we find the overall distribution of MT stiffness to be broad and non-Gaussian, so we characterize the filament stiffness at each condition by the median value and indicate the percentile differences in the distributions using a box and whiskers plot format [Hawkins et al., 2012]. As shown in Fig. 2, in the absence of tau we find MTs stabilized by epothilone compounds are substantially softer than are MTs stabilized by taxol. The median L_p value for taxol-stabilized MTs is 2.0 mm, whereas MTs stabilized by epothilone-A or epothilone-B have median L_p values of 1.6 and 1.2 mm, respectively. For MTs stabilized by taxol or epothilone-A, the addition of either 3R or 4R tau at a 5:1 molar ratio of tubulin:tau

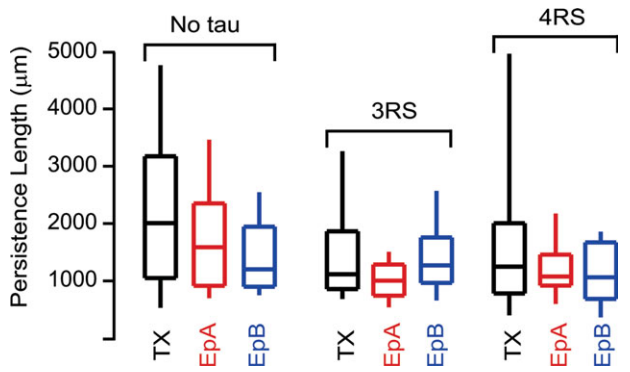

Fig. 2. MT stiffness as a function of stabilization condition and tau. MT stiffness is determined from the spectrum of thermal fluctuations of freely diffusing filaments. MTs are stabilized by either epothilone-A, epothilone-B, or taxol, then coated with no tau, 100 nM 3R tau, or 100 nM 4R tau. Under each condition, we find the distribution in stiffness determined from an ensemble of different MTs (N = 25–78). Box and whiskers plots are constructed as follows: The middle line of each box represents the median, the upper box edge represents the 75th percentile, the lower box edge represents the 25th percentile, and the upper and lower whisker extensions represent the 90th and 10th percentiles, respectively. Raw data distributions are shown in Supporting Figure S1.

softens the filaments. The median persistence length of epothilone-A-stabilized MTs drops to 1.0 mm for 3R tau (~37% reduction) and 1.1 mm for 4R tau (~31% reduction). The median persistence length of taxol-stabilized MTs drops to 1.1 mm for 3R tau (~45% reduction) and 1.3 mm for 4R tau (~35% reduction). By contrast, for epothilone-B-stabilized MTs, the addition of tau has little effect: the median L_p of the epothilone-B-stabilized MTs increases slightly to 1.3 mm for 3R tau and decreases to 1.1 mm for 4R tau (~8% increase or reduction, respectively). Interestingly, although we find the stiffness of the bare MTs varies substantially depending on the type of small molecule used, upon addition of either 3R or 4R tau, these differences nearly vanish.

Effects of Small-Molecule Stabilizers and Tau on Kinesin Translocation

We next assessed the ability of MTs stabilized with epothilone-A or epothilone-B to support kinesin motility, and further, tested the effects of 3R or 4R tau proteins on kinesin translocation for each polymerization condition. These measurements are motivated by a desire to determine the functionality of epothilone-stabilized MTs, particularly with regard to axonal transport, since transport defects have been linked to CIPN. We employ a quantum-dot (QD)-based motility assay, in which small numbers of kinesin motors are bound to fluorescent QDs in a manner that mimics in vivo cargo attachment. Given the system geometry and kinesin concentrations, we estimate that there will be, on average, 2–3 MT-bound kinesin molecules per QD.

We measured the velocity of the kinesin-QD complexes moving on MTs assembled with epothilone-A, epothilone-B, or taxol, then coated with no tau, 100 nM 3R tau, or 100 nM 4R tau. In the absence of tau proteins, we find no significant difference between the speed of kinesin motors moving on MTs stabilized by taxol or epothilone-A; kinesins moving on epothilone-B-stabilized MTs show a modest, but statistically significant slowing with respect to the taxol MTs (Fig. 3). The differences between the speeds of kinesins moving on MTs polymerized with epothilone-A or epothilone-B are not significant at the 95% confidence level. Full statistical analysis of the velocity data is given in Table II.

We find a substantial slowing when we introduce tau. In separate experiments, we found that, the addition of either 3R or 4R tau to taxol-stabilized MTs reduces the mean kinesin speed from 425 ± 10 nm/s (errors given by SEM) to 360 ± 15 nm/s (~15% reduction) or 334 ± 20 (~21% reduction), respectively (Yu et al., unpublished observations). For both isoforms, the tau-dependent velocity reduction is significant ($P < 0.001$), whereas the differences in mean speed between the two isoforms (3R versus 4R) is not.

We also find significant tau-dependent reductions in kinesin speed when using MTs polymerized with either

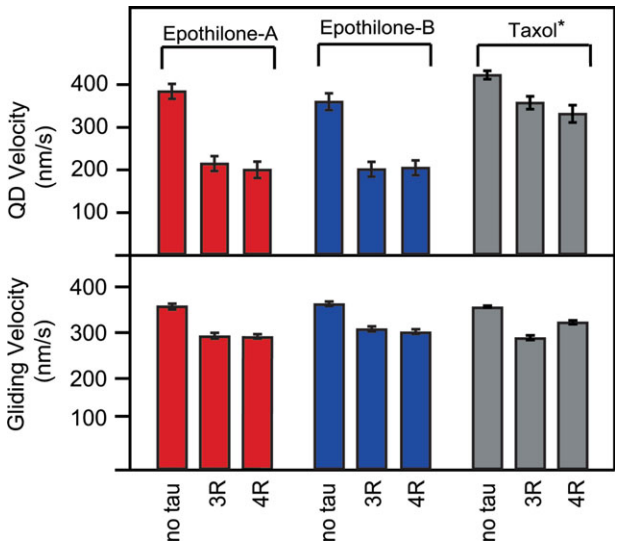

Fig. 3. Kinesin velocity as a function of stabilization condition and tau. Kinesin velocity is determined using a MT gliding assay (upper panel, $N = 72–354$) or QD assay (lower panel, $N = 22–93$). MTs are stabilized by epothilone-A, epothilone-B, or taxol, then coated with no tau, 3R tau, or 4R tau. Full statistical analysis of these data is given in Table II. Error bars are SEM. *Previously reported values (Yu et al., unpublished observations). Raw data distributions are shown in Supporting Figures S2 and S3.

epothilone-A or epothilone-B, and moreover find that the magnitude of the reduction is significantly larger than that observed when using taxol-stabilized MTs. When using epothilone-A-stabilized MTs, the addition of 3R reduces the mean kinesin speed from 387 ± 17 to 218 ± 17 nm/s (~44% reduction) and the addition of 4R tau reduces the mean kinesin speed to 203 ± 17 nm/s (~48% reduction). When using epothilone-B-stabilized MTs, the addition of 3R reduces the mean kinesin speed from 362 ± 20 to 204 ± 17 nm/s (~44% reduction) and the addition of 4R tau reduces the mean kinesin speed to 208 ± 18 nm/s (~43% reduction). For MTs stabilized with either epothilone compound, reductions in velocity upon addition of either tau isoform are significant ($P < 0.001$). However, we do not find any significant epothilone compound-specific differences when the tau type and concentration is fixed, and we do not find tau-isoform specific differences when either epothilone-A or -B are used.

Another common measure of kinesin function in single molecule in vitro assays is the total travel distance per diffusional encounter with the MT, or "run length." By contrast, in our assay, each QD accommodates a small number of kinesin motors, and thus the cargo run length is not a particularly useful metric. In the limit that each motor operates independently, the probability of detachment of cargo from the MT depends on the product of detachment probabilities of each motor. In the case of single kinesin motors moving along bare taxol-stabilized MTs, the probability of detachment is $\sim 10^{-2}$ per step. Given an 8-nm step size, this leads to an average run

Table II. Results of Statistical Analysis of Velocity Data

		QD Assay		Gliding Assay	
Condition 1	Condition 2	*h*	*P*-value	*h*	*P*-value
EpA	EpB	0		0	
EpA	TX	0		0	
EpB	TX	1	$P<0.01$	0	
EpA 3RS	**EpA**	**1**	***P* <0.001**	**1**	***P*<0.001**
EpA 4RS	**EpA**	**1**	***P* <0.001**	**1**	***P*<0.001**
EpB 3RS	**EpB**	**1**	***P* <0.001**	**1**	***P*<0.001**
EpB 4RS	**EpB**	**1**	***P* <0.001**	**1**	***P*<0.001**
EpA 3RS	EpB 3RS	0		1	$P<0.05$
EpA 4RS	EpB 4RS	0		0	
EpB 3RS	**TX 3RS**	**1**	***P*<0.001**	**1**	***P*<0.01**
EpB 4RS	**TX 4RS**	**1**	***P* <0.001**	**1**	***P*<0.001**
EpA 3RS	TX 3RS	1	$P<0.001$	0	
EpA 4RS	**TX 4RS**	**1**	***P* <0.001**	**1**	***P*<0.001**
EpA 3RS	EpA 4RS	0		0	
EpB 3RS	EpB 4RS	0		0	

A two-sample Student's *t*-test (implemented in MATLAB) is used to compare the velocity data for both the QD and gliding assay to identify statistically-significant differences in kinesin translocation rates. An *h* value of 1 indicates a significant difference at a minimum confidence level of 95%. *P* value ranges are shown for data where $h = 1$. Those conditions that were found to be significantly different using both assays are indicated in bold. The labels at each condition give the type of small molecule stabilizer used (EpA = Epothilone-A, EpB = Epothilone-B, TX = taxol), the type of tau protein used (3R or 4R), and the molar ratio of tubulin dimer:tau in the original mixture.

length of ~800 nm. When two motors are simultaneously engaged, the predicted run length increases to 80 μm, much longer than the average MT length used in our studies. Consistent with this, in the absence of tau, >90% of the kinesin-QD assemblies bind and translocate to the end of MTs assembled by either epothilone compound or taxol. The observed run length is given by one-half of the average MT length and this is a substantial underestimate of the actual run length of the assembly. In the presence of tau, the percentage of kinesin-QD assemblies that bind and move to the end of the MT drops to ~50%, and the mean value of run length also decreases, but we do not find any obvious trend with type of stabilizing compound used (data not shown).

To confirm the results of our QD assay in a different experimental geometry, we repeated these measurements using MT gliding assays, in which fluorescently labeled MTs glide on top of a densely kinesin-coated surface. Multiple kinesin motors bind along the length of the filament and each steps toward the MT plus end, thereby propelling the MT across the surface. The velocity measured from the gliding assays will thus be an average velocity driven by the collective behavior of all active motors. As shown in Fig. 3 and Table II, the data obtained with the gliding assay format follow the same overall trends as those obtained with the QD assay. In the absence of tau, we find no significant differences in MT velocity when epothilone-A, epothilone-B, or taxol are used. We find a significant velocity reduction when either tau isoform is added to MTs stabilized with either epothilone compound at a tubulin:tau ratio of 5:1. The speed reductions are smaller as compared to those measured using the QD assay, with tau-dependent reductions of ~15–18%, in contrast to the 43–48% reductions we observed with the QD assay. When compared to the velocities at which tau-coated taxol-stabilized MTs move, we again measure smaller differences than were observed with the QD assay. We find significant reductions in gliding velocities of MTs coated with the 4R tau isoform for both epothilone compounds ($P < 0.001$). For the 3R tau isoform, we find even smaller differences between the speeds of MTs stabilized with either epothilone compound and taxol. When the MTs are coated with 3R tau, the reduction in gliding velocities for epothilone-A-stabilized MTs as compared to taxol-stabilized MTs is significant, although the *P*-value is larger ($P < 0.01$); for 3R tau coated MTs, the velocity difference between the taxol-stabilized MTs and epothilone-B-stabilized MTs is not significant.

Discussion

There have been several prior studies of the effects of tau on MT stiffness. In the absence of small molecule stabilizers, MTs that have been polymerized in the presence of GTP with GMPCPP stabilizing caps were measured to have a mean L_p of ~6.0 mm at 37°C using a similar spectral analysis method [Mickey and Howard, 1995]. For MTs that are polymerized in the presence of taxol without GMPCPP caps, the mean L_p has been measured by spectral analysis to be 7.5 mm at 37°C and 4.9 mm at 25°C [Gittes et al., 1993; Mickey and Howard, 1995]. The stiffness of MTs polymerized in the presence of a recombinant bovine tau protein with four binding repeats and two projection domains at a molar ratio of ~5:1 tubulin:-tau, but without small molecule stabilizers, was determined to be 7.9 mm [Mickey and Howard, 1995].

A second prior approach examined the shape changes of MTs that are actively bent using optical tweezers and then allowed to relax back to their equilibrium shape by moving through a viscous buffer [Felgner et al., 1996; Felgner et al., 1997]. Using this relaxation method, the persistence length of MTs grown off an axoneme template under various polymerization conditions was determined for MTs at room temperature (22–25°C). In the absence of stabilizing compounds or tau, the mean L_p was measured to be 0.9 mm, and in the presence of taxol this value decreases to 0.2 mm [Felgner et al., 1996]. Although there

are significant variations in the stiffness values determined by different methods [as reviewed in Hawkins et al., 2010], the hydrodynamic relaxation methods tend to give systematically lower values for stiffness than do the methods that employ spectral analysis of thermal fluctuations. The role of taxol in determining MT stiffness has been particularly controversial, although most measurements have indicated that the addition of taxol softens MTs [Hawkins et al., 2010]. Consistent with this, we have found that the addition of taxol to GMPCPP-stabilized MTs reduces MT stiffness (data not shown).

To our knowledge, there have been no measurements of the effects of epothilone compounds on MT stiffness, however, a number of structural studies have indicated that epothilone binding induces tubulin conformational changes. Hydrogen-deuterium exchange mass spectroscopy experiments have shown that epothilone-A, epothilone-B, and a synthetic analog of epothilone-B called ixabepilone improve longitudinal contacts at the interface between tubulin dimers along a single protofilament and have little effect on the lateral interactions between protofilaments [Huzil et al., 2008; Khrapunovich-Baine et al., 2011]. Similar interactions were observed when MTs were stabilized by docetaxel, a compound related to taxol [Huzil et al., 2008]. The epothilones and taxol appear to bind to the same (or overlapping) sites on the tubulin dimer and to stabilize MTs in a similar manner [Correia and Lobert, 2001]. MTs stabilized by either taxol or epothilone-B have been found to have similar architecture, with the epothilone-stabilized MTs being slighter larger in diameter: 60% or 35% of taxol-stabilized MTs have 12 or 13 protofilaments, whereas 22% or 67% of epothilone-B-stabilized MTs have 12 or 13 protofilaments, respectively [Meurer-Grob et al., 2001]. Given this, the origins of decreased stiffness with the epothilone compounds are not clear.

In the absence of small molecule stabilizers, the addition of a wide variety of tau constructs uniformly increased MT stiffness, as measured by hydrodynamic relaxation [Felgner et al., 1997]. When MTs were assembled with the tau construct most similar to our 3R tau (the HT23 construct with three MT binding repeats and zero projection domains) the mean L_p value increased from 0.9 to 2.1 mm when the MT surface was nearly saturated with tau. When a four-repeat tau construct with two projection domains (the HT40 construct, or the "long" form of 4R tau) was used at a concentration near MT saturation, the MT L_p was 2.5 mm. When the concentration of HT40 was systematically increased from ~2% to ~85% of saturation, the measured L_p values increased monotonically.

Our results extend this prior work in two ways. After confirming that MTs stabilized by both epothilone-A and -B were able to bind tau proteins at affinities that were similar to taxol-stabilized MTs, we determined the effects of these non-taxol small molecule stabilizers on MT stiffness. We find that in the absence of tau proteins, epothilone-stabilized MTs are substantially less stiff than those stabilized by taxol, and that epothilone-A- and -B-stabilized MTs have slightly different stiffnesses. Of all three stabilizing compounds, epothilone-B MTs are most flexible. When we add either the 3R or 4R "short" tau constructs, to the taxol- or epothilone-A-stabilized MTs, the stiffness decreases. For epothilone-B stabilized MTs, there is no clear effect with the addition of tau. This is in contrast to prior work on MTs assembled by tau in the absence of stabilizing drugs, in which the addition of tau proteins has always increased stiffness. Interestingly, the stiffness differences that we observed using MTs formed by different stabilizing compounds in the absence of tau nearly vanish.

The molecular-level changes that give rise to this tau-dependent reduction in stiffness in the presence of small-molecule stabilizers are not clear. Possible mechanisms include either a reduction in the number of protofilaments upon addition of tau, or a change in the interprotofilament or intraprotofilament interaction energy that would lead to a reduction in the effective bending modulus of the MT. For the case of taxol-stabilized MTs, the addition of any of the six naturally occuring isoforms of tau has been shown to increase the average MT protofilament number in a tau concentration-dependent manner [Choi et al., 2009]. This suggests that at least for taxol-stabilized MTs, the reduction in stiffness due to tau addition must arise from changes in the interaction energies between tubulin dimers. To our knowledge, the effects of epothilone compounds on MT structure in the presence of tau are unknown.

We also tested the ability of epothilone-stabilized MTs to support kinesin translocation using two experimental geometries in the QD and MT gliding motility assays. In the absence of tau, both epothilone-A and -B are able to support kinesin-driven motility, at speeds that are similar to and in most cases indistinguishable from that of taxol-stabilized MTs. For all small molecule stabilizers, we find that the addition of tau decreases kinesin velocity. In almost all cases, the reductions observed are greater when MTs are stabilized with an epothilone compound rather than taxol. The tau-dependent reductions are markedly larger for the epothilone compounds when the QD assay is used.

We suspect that the origins of these differences arise due to the different binding geometries in the QD and gliding assays. In the MT gliding assay, large ensembles of kinesin motors work cooperatively to move a MT, whereas in the QD assay only 2–3 kinesin motors are actively engaged at any one time. It is possible that the topography of the epothilone-stabilized MTs differs from that of the taxol-stabilized MTs in a manner that causes the kinesin motors to adopt different trajectories along the surface.

Since the QD assay averages the motions of a small number of motors, any instantaneous changes in stepping patterns due either to direct tau-kinesin interactions, or tau-dependent differences in the tubulin-kinesin interactions may be more evident in the QD assay than in the MT gliding assay that averages over a much larger ensemble.

Alternatively, it is possible that the differences observed using the MT gliding and QD assays arise from subtle changes in tau concentration in the two assays. The multiple wash steps and buffer exchanges used in the preparation of the immobilized MTs and kinesin-QD complexes prevent knowledge of the absolute tubulin:tau molar ratio, whereas the MT gliding assay maintains a well-defined tubulin:tau ratio of 5:1. However, we have tested the effects of tau concentration on kinesin translocation using taxol-stabilized MTs and found no change in velocity for tau concentrations ranging from 100 nM to 1 μM, consistent with prior results. Moreover, the QD assay preparation is identical for MTs polymerized with each small molecule stabilizer, and we control the average number of MTs per field of view for each experiment. Thus, even if some of the differences we observe between the QD and MT gliding assays do arise from changes in bound tau concentration, we expect that the differences observed between the taxol- and epothilone-stabilized MTs using the QD assay do not.

In summary, we find the MTs stabilized by either epothilone-A or epothilone-B are competent to bind tau proteins and support kinesin translocation. However, epothilone-stabilized MTs are substantially less stiff than taxol-stabilized MTs, and the addition of tau proteins to MTs stabilized by either epothilone-A or taxol further reduces stiffness. Kinesin translocation is also affected not only by the presence of tau but also by the type of small molecule stabilizer used. These results suggest that small molecule stabilizers do not simply stabilize a "native" MT structure but rather are active agents that remodel MT structure, function, and mechanics. This may have important consequences to the use of these agents as chemotherapeutics. One possible outcome of our work is the development of functional screening methods to select and optimize chemotherapeutic compounds with minimal impacts on MT stiffness, kinesin translocation, and axonal transport.

Materials and Methods

Tubulin Preparation and MT Assembly

MAP-free tubulin dimers (>99% pure) were purified from bovine brain without stabilizing agents as previously described [Miller and Wilson, 2010]. Briefly, tubulin was purified from brain homogenates by two cycles of polymerization and depolymerization, followed by elution through a phosphocellulose column. Rhodamine-labeled tubulin (0.14 mole rhodamine per mole tubulin) was prepared as described [Hyman et al., 1991]. MTs were prepared by mixing 20 μM of MAP-free tubulin and rhodamine-labeled tubulin mixed at a molar ratio of 5:1, with taxol, epothilone-A or epothilone-B (Sigma Aldrich) in PEM-80 buffer (80 mM PIPES, 1 mM EGTA, 4 mM $MgCl_2$, pH 6.9) supplemented with β-mercaptoethanol and 2 mM of GTP. MTs were assembled at 35°C with an initial 10 min incubation, then epothilone-A, epothilone-B, or taxol was introduced in three steps, to a concentration of 1 μM, then 6.5 μM, then 20 μM (final) with 20 min waiting periods between each addition (total reaction time is 70 min). This step-wise addition is commonly used when generating taxol-assembled MTs to prevent formation of non-MT structures and promote long MTs [Thompson et al., 1981]. The total tubulin concentration in the resulting stock MT solution is 20 μM.

Protein Expression and Purification

The kinesin construct (K560-CL-his) was a gift from Dr. Ron Vale (UCSF). In a pET expression vector, the cDNA encodes the N-terminal 560 amino acids of human conventional kinesin heavy-chain that lacks solvent exposed cysteines but retains normal enzymatic and motile properties [Rice et al., 1999]. A C-terminal hexa-histadine cluster allows for Ni-affinity purification. K560-CL-his was expressed in BL21 (DE3) cells (Invitrogen) and purified as previously described [Peck et al., 2011]. When prepared for use with quantum dots, the purified kinesin proteins were subsequently labeled with EZ-Link® Maleimide-PEG2-Biotin (Thermo Scientific) via maleimide-thiol coupling. In both cases, kinesin was concentrated, supplemented with 10% sucrose and 0.1 mM ATP, drop frozen in liquid nitrogen in single-use aliquots, and stored at −80°C.

Tau-encoding plasmids and expressed proteins were a gift of Dr. Stuart Feinstein, UCSB. Tau (>99% pure) was recombinantly produced using pRK expression vectors containing cDNA sequences encoding 3-repeat or 4-repeat human tau containing no N-terminal inserts (which we refer to as 3R or 4R tau herein). Recombinant tau was purified as previously described except that the final purification steps consisted of a HiTrap Phenyl HP column (GE Healthcare) followed by dialysis into BRB-80 buffer (80 mM PIPES, 1 mM EGTA, 1 mM $MgSO_4$, pH 6.8) supplemented with 0.1% β-mercaptoethanol [Levy et al., 2005]. The concentration of purified tau was determined by quantitative SDS-PAGE, through comparison with a tau mass standard [Panda et al., 2003].

Tau-MT Cosedimentation Assays

Cosedimentation assays were used to determine the amount of bound tau under each polymerization condition. Here, MTs were formed as described. 3R or 4R tau were added at

a molar ratio of 5:1 or 30:1 tubulin dimer:tau, and the reaction allowed to continue for an additional 15 min at room temperature. In detail, we used 3 and 0.5 μM of tau and added the appropriate amount of MTs based on the tau:tubulin ratio. Tau-coated MTs were layered over 180 μL of a warm sucrose cushion (50% w/v in PEM-80, supplemented with 2 mM GTP) in a 5 × 20 mm UltraClear centrifuge tube (Beckman Coulter). Samples were spun in a TLA 100.3 fixed angle rotor for 12 min at 60,000 rpm (194,000×*g*) at 35°C. Supernatants and pellets were collected and solubilized in SDS-PAGE sample buffer. The quantities of tau and tubulin in each were determined by Western blotting using the monoclonal antibody Tau-1 (Millipore) and Coomassie blue staining, respectively, taking care to operate within the linear detection range. Negligible quantities of tau or tubulin remained within the cushion. These data were used to determine the molar ratio of tubulin to tau in the MT pellet.

Kinesin-driven MT Gliding Assays

Gliding assays were performed as previously described, with minor modifications [Peck et al., 2011]. Flow-chambers were constructed by attaching a coverslip to a glass slide with double-sided tape. Prior to use, coverslips were cleaned by exposure to a gas plasma generated by exposing room air to an 18 W radio frequency oscillating field for 10 min at pressure of ∼0.5–2 Torr using a commercial benchtop plasma cleaner (Harrick PDC-32G). Kinesin was diluted to 20–50 μg/mL in PEM80 buffer containing 10 mM β-mercaptoethanol then flowed into the chamber and allowed to directly adhere to the glass surface for 3 min. Following attachment of motors, the chamber was incubated for an additional 5 min with a solution of casein (∼0.5 mg/mL) to reduce the nonspecific binding of MTs to the glass surfaces. MTs were polymerized as described and used within 24 h. For experiments with tau protein, 3R or 4R tau was added to a final ratio of 5:1 tubulin to tau. For measurements without tau protein, an equivalent volume of warm buffer was added to ensure similar final MT concentrations. In all cases, the MTs were incubated at 35°C for another 15 min, and the solution was diluted 1:100 in warm motility buffer containing PEM-80, 5 mM ATP, 0.1% β-mercaptoethanol and an enzymatic oxygen scavenger system (650 U/mL catalase, 15 U/mL glucose oxidase, and 4.5 mg/mL glucose, final concentrations). The diluted MTs were flowed into the kinesin-containing flow chamber, which was sealed with vacuum grease and visualized immediately. Gliding events were visualized using a Nikon Ti-S microscope equipped with custom-built total internal reflection fluorescence (TIRF) illumination capabilities (67 nm/pixel, and 19–20°C ambient temperature). Excitation wavelength used for rhodamine imaging was 532 nm. Images were collected using an air-cooled EMCCD camera (Andor, iXon) every 0.4 s for 100 frames. MT tracking was performed manually using ImageJ to identify the leading tip of the moving MT in each frame. To calculate velocity, the total MT trajectory was divided by the time interval over which motion was observed.

Kinesin-driven QD Assays

The epothilone-stabilized MTs used in the QD assays were generated as described with an extra centrifugation step (14 krpm, 10 min) to remove unpolymerized tubulin dimers, which contribute to background fluorescence. The pellet was gently resuspended in a stabilization buffer containing 1 mM GTP, 2 μM epothilone-A or epothilone-B, 1 mM DTT and 2 μg of sodium azide in PEM-80, and stored at room temperature, away from light. MTs formed by this method are typically stable for up to 1 week. QD assays were performed as previously described, with modifications [Yildiz et al., 2008]. Glass flow chambers were constructed by attaching plasma cleaned 22 × 40 mm #1.5 coverslips to clean glass microscope slides with two parallel pieces of double-sided tape spaced ∼5 mm apart. β tubulin antibody (SC-58884, Santa Cruz Biotechnology Inc.) solution (40 μg/mL) was flowed into the chambers to allow absorption to the coverslip surface. After 10 min, excess antibodies were washed out by addition of 50 μL of PEM-80. The stock MT solution was diluted 1:20 in PEM-80, and 20 μL of diluted MT solution was flowed into the chambers. After a 10 min incubation period, 4 mg/mL casein solution was introduced to remove the unattached MTs and to passivate the glass surfaces against nonspecific adsorption of kinesin or tau. After 10 min, biotinylated kinesins, diluted to ∼20 ng/mL in a solution of PEM-80 supplemented with 1 mM AMPPNP, were introduced to the flow chamber. After 5 min, chambers were washed and Qdot® 605 steptavidin conjugated quantum dots (Q10101 MP, Invitrogen), diluted to 0.2 nM in PEM-80 were introduced. After another 5 min, chambers were washed with a standard motility buffer for single-molecule kinesin measurements, consisting of PEM-80 supplemented with 5 mM DTT, 1% β-mercaptoethanol, an enzymatic oxygen scavenger system (650 U/mL catalase, 15 U/mL glucose oxidase and 4.5 mg/mL glucose, final concentrations), 1 mM ATP, and the desired type of tau protein at a final concentration of 100 nM tau. The chambers were sealed with vacuum grease and visualized immediately at room temperature (19–20°C). Under these assembly conditions, the polymerized tubulin dimer to kinesin dimer molar ratio in the microchamber is approximately 25:1. Considering the cylindrical geometry of the MT and the size of the QD there will be, on average, 2–3 MT-bound kinesin molecules accessible to any QD that diffuses near a MT.

Motions of single QDs were visualized using a custom-built TIRF microscope (magnification = 67 nm/pixel).

Images were collected at room temperature using an air-cooled EMCCD camera (Andor, iXon) at a rate of 10 frames per second. Excitation wavelength for QD imaging was 488 nm. A broadband emission filter was selected to allow the dim outline of the rhodamine-labeled MT to be observed in the background of the bright QD images. Images were analyzed off-line after data collection. Movies were manually screened to identify the motion of kinesin-driven QDs that warranted velocity analysis. Only runs that persisted for at least 30 frames were analyzed. QD position was determined as a function of time using the built-in FIONA algorithm available through Video Spot Tracker software (made available by CISMM at UNC-CH, supported by the NIH NIBIB, Award# NIH 5-P41-RR02170). The initial velocities of the kinesin-QD assemblies were calculated framewise then refined to discriminate between motions parallel or perpendicular to the MT axis using a graphic-based analysis algorithm implemented in MATLAB. This was particularly useful for cases in which tau binding disrupted the antibody-MT connection, leading to thermal fluctuations of the MT substrate upon which the kinesin motors walk. For each moving kinesin-QD assembly, a region with a width of 15 pixels was drawn around the average location of the underlying MT track. The MT location was then determined by fitting a Gaussian curve to the cross section of intensity of the MT contour using ~100 evenly distributed points, as previously described [Valdman et al., 2012]. Curve fitting was implemented using built-in algorithms. Using the resulting MT coordinates, the initial velocities were projected into two orthogonal components, one parallel and one perpendicular to the MT contour. The kinesin velocity for a single translocation event (i.e., a "run") was given by the mean of the parallel components of the framewise velocities.

MT Fluctuation Assays

Epothilone-assembled MTs were diluted into a PEM-80 based solution supplemented with 5 mM DTT, 1% β-mercaptoethanol with oxygen scavenger system (glucose oxidase, catalase, glucose) and 1–5 mg/mL casein. For experiments with taxol-assembled MTs, the solution is supplemented with 10 μM taxol. A drop of 2.6 μL of the MT solution is pipetted onto a clean glass slide, and a plasma-cleaned 22 × 40 mm^2 #1.5 cover glass is placed on top. Gentle pressure is applied to spread the solution over the entire surface of the cover glass, resulting in a distance between the glass surfaces of ~3 μm. The chamber is sealed with VALAP wax (equal parts Vaseline, lanolin, and paraffin) to prevent convection and Vaporation. The sample is observed immediately using the custom-built TIRF microscope and images collected using an air cooled EMCCD camera at a rate of 10 frames per second. For these measurements, we set the incident angle for laser injection to be slightly below the critical angle for true total internal reflection. This allows a mixed mode TIRF/epi excitation that allows visualization of the filaments throughout the depth of the observation chamber. Magnification is 67 nm/pixel, and data are collected at room temperature (19–20°C). A movie of 300–400 frames was collected for each fluctuating MT and was analyzed using a custom-designed tracing and spectral analysis method, as described [Valdman et al., 2012].

Acknowledgment

The authors thank Dr. Ron Vale (UCSF) and Dr. Stuart Feinstein (UCSB) for providing the kinesin and tau plasmids, respectively, Herb Miller and Leslie Wilson for providing purified tubulin, and Elmer Guzman for assistance in preparing various tau constructs. They thank Nichole LaPointe, Benjamin Lopez, David Valdman, and Paul Atzberger for technical assistance and helpful comments. The authors also gratefully acknowledge support from a Burroughs Wellcome Fund Career Award at the Scientific Interface, a University of California Cancer Research Coordinating Committee Award, and support from the UCSB Materials Research Laboratory Research Internships in Science and Engineering (RISE) program through the NSF MRSEC grant DMR-1121053. Authors declare that they have no conflicts of interest.

References

Alvarez RH, Valero V, Hortobagyi GN. 2011. Ixabepilone for the treatment of breast cancer. Ann Med 43(6):477–486.

Argyriou AA, Koltzenburg M, Polychronopoulos P, Papapetropoulos S, Kalofonos HP. 2008. Peripheral nerve damage associated with administration of taxanes in patients with cancer. Crit Rev Oncol/Hematol 66:218–228.

Binder LI, Frankfurter A, Rebhun LI. 1985. The distribution of tau in the mammalian central nervous system. J Cell Biol 101(4):1371–1378.

Block SM, Asbury CL, Shaevitz JW, Lang MJ. 2003. Probing the kinesin reaction cycle with a 2D optical force clamp. Proc Natl Acad Sci 100(5):2351–2356.

Bollag DM, McQueney PA, Zhu J, Hensens O, Koupal L, Liesch J, Goetz M, Lazarides E, Woods CM. 1995. Epothilones, a new class of microtubule-stabilizing agents with a taxol-like mechanism of action. Cancer Res 55(11):2325–2333.

Chen J, Kanai Y, Cowan NJ, Hirokawa N. 1992. Projection domains of MAP2 and tau determine spacings between microtubules in dendrites and axons. Nature 360(6405):674–677.

Choi MC, Raviv U, Miller HP, Gaylord MR, Kiris E, Ventimiglia D, Needleman DJ, Kim MW, Wilson L, Feinstein SC, et al. 2009. Human microtubule-associated-protein tau regulates the number of protofilaments in microtubules: a synchrotron x-ray scattering study. Biophys J 97(2):519–527.

Correia JJ, Lobert S. 2001. Physiochemical aspects of tubulin-interacting antimitotic drugs. Curr Pharm Des 7(13):1213–1228.

Cortes J, Baselga J. 2007. Targeting the microtubules in breast cancer beyond taxanes: the epothilones. Oncologist 12:271–280.

Dixit R, Ross JL, Goldman YE, Holzbaur EL. 2008. Differential regulation of dynein and kinesin motor proteins by tau. Science 319(5866):1086–1089.

Drubin DG, Feinstein SC, Shooter EM, Kirschner MW. 1985. Nerve growth factor-induced neurite outgrowth in PC12 cells involves the coordinate induction of microtubule assembly and assembly-promoting factors. J Cell Biol 101(5 Pt 1):1799–1807.

Ebneth A, Godemann R, Stamer K, Illenberger S, Trinczek B, Mandelkow E. 1998. Overexpression of tau protein inhibits kinesin-dependent trafficking of vesicles, mitochondria, and endoplasmic reticulum: implications for Alzheimer's disease. J Cell Biol 143(3):777–794.

Feinstein SC, Wilson L. 2005. Inability of tau to properly regulate neuronal microtubule dynamics: a loss-of-function mechanism by which tau might mediate neuronal cell death. Biochim Biophys Acta 1739(2–3):268–279.

Felgner H, Frank R, Schliwa M. 1996. Flexural rigidity of microtubules measured with the use of optical tweezers. J Cell Sci 109(Pt 2):509–516.

Felgner H, Frank R, Biernat J, Mandelkow EM, Mandelkow E, Ludin B, Matus A, Schliwa M. 1997. Domains of neuronal microtubule-associated proteins and flexural rigidity of microtubules. J Cell Biol 138(5):1067–1075.

Ferreira A, Niclas J, Vale RD, Banker G, Kosik KS. 1992. Suppression of kinesin expression in cultured hippocampal neurons using antisense oligonucleotides. J Cell Biol 117(3):595–606.

Gittes F, Mickey B, Nettleton J, Howard J. 1993. Flexural rigidity of microtubules and actin filaments measured from thermal fluctuations in shape. J Cell Biol 120(4):923–934.

Hagiwara H, Sunada Y. 2004. Mechanism of taxane neurotoxicity. Breast Cancer 11(1):82–85.

Hawkins T, Mirigian M, Selcuk Yasar M, Ross JL. 2010. Mechanics of microtubules. J Biomech 43(1):23–30.

Hawkins T, Mirigian M, Li J, Yasar M, Sackett D, Sept D, Ross J. 2012. Perturbations in microtubule mechanics from tubulin preparation. Cell Mol Bioeng 5(2):227–238.

Himmler A. 1989. Structure of the bovine tau gene: alternatively spliced transcripts generate a protein family. Mol Cell Biol 9(4): 1389–1396.

Himmler A, Drechsel D, Kirschner MW, Martin DW Jr. 1989. Tau consists of a set of proteins with repeated C-terminal microtubule-binding domains and variable N-terminal domains. Mol Cell Biol 9(4):1381–1388.

Hirokawa N, Shiomura Y, Okabe S. 1988. Tau proteins: the molecular structure and mode of binding on microtubules. J Cell Biol 107(4):1449–1459.

Hurd DD, Stern M, Saxton WM. 1996. Mutation of the axonal transport motor kinesin enhances paralytic and suppresses Shaker in *Drosophila*. Genetics 142(1):195–204.

Huzil JT, Chik JK, Slysz GW, Freedman H, Tuszynski J, Taylor RE, Sackett DL, Schriemer DC. 2008. A unique mode of microtubule stabilization induced by peloruside A. J Mol Biol 378(5):1016–1030.

Hyman A, Drechsel D, Kellogg D, Salser S, Sawin K, Steffen P, Wordeman L, Mitchison T. 1991. Preparation of modified tubulins. Methods Enzymol 196:478–485.

Khrapunovich-Baine M, Menon V, Yang C-PH, Northcote PT, Miller JH, Angeletti RH, Fiser A, Horwitz SB, Xiao H. 2011. Hallmarks of molecular action of microtubule stabilizing agents. J Biol Chem 286(13):11765–11778.

Kieran D, Hafezparast M, Bohnert S, Dick JR, Martin J, Schiavo G, Fisher EM, Greensmith L. 2005. A mutation in dynein rescues axonal transport defects and extends the life span of ALS mice. J Cell Biol 169(4):561–567.

LaMonte BH, Wallace KE, Holloway BA, Shelly SS, Ascano J, Tokito M, Van Winkle T, Howland DS, Holzbaur EL. 2002. Disruption of dynein/dynactin inhibits axonal transport in motor neurons causing late-onset progressive degeneration. Neuron 34(5):715–727.

Lee G, Cowan N, Kirschner M. 1988. The primary structure and heterogeneity of tau protein from mouse brain. Science 239(4837):285–288.

Lema MJ, Foley KM, Hausheer FH. 2010. Types and epidemiology of cancer-related neuropathic pain: the intersection of cancer pain and neuropathic pain. Oncologist 15:3–8.

Levy SF, Leboeuf AC, Massie MR, Jordan MA, Wilson L, Feinstein SC. 2005. Three- and four-repeat tau regulate the dynamic instability of two distinct microtubule subpopulations in qualitatively different manners. Implications for neurodegeneration. J Biol Chem 280(14):13520–13528.

Mandelkow EM, Stamer K, Vogel R, Thies E, Mandelkow E. 2003. Clogging of axons by tau, inhibition of axonal traffic and starvation of synapses. Neurobiol Aging 24(8):1079–1085.

Meurer-Grob P, Kasparian JRM, Wade RH. 2001. Microtubule structure at improved resolution. Biochemistry 40(27):8000–8008.

Mickey B, Howard J. 1995. Rigidity of microtubules is increased by stabilizing agents. J Cell Biol 130(4):909–917.

Miller HP, Wilson L. 2010. Preparation of microtubule protein and purified tubulin from bovine brain by cycles of assembly and disassembly and phosphocellulose chromatography. In: Wilson L, Correia JJ, editors. Methods in Cell Biology. Elsevier Inc. pp 3–15.

Panda D, Samuel JC, Massie M, Feinstein SC, Wilson L. 2003. Differential regulation of microtubule dynamics by three- and four-repeat tau: implications for the onset of neurodegenerative disease. Proc Natl Acad Sci USA 100(16):9548–9553.

Park SB, Krishnan AV, Lin CS-Y, Goldstein D, Friedlander M, Kiernan MC. 2008. Mechanisms underlying chemotherapy-induced neurotoxicity and the potential for neuroprotective strategies. Curr Med Chem 15:3081–3094.

Park SB, Lin CS-Y, Krishnan AV, Friedlander ML, Lewis CR, Kiernan MC. 2011. Early, progressive, and sustained dysfunctoin of sensory axons underlies paclitaxel-induced neuropathy. Muscle Nerve 43:367–374.

Peck A, Sargin ME, LaPointe NE, Rose K, Manjunath BS, Feinstein SC, Wilson L. 2011. Tau isoform-specific modulation of kinesin-driven microtubule gliding rates and trajectories as determined with tau-stabilized microtubules. Cytoskeleton 68(1):44–55.

Rice S, Lin AW, Safer D, Hart CL, Naber N, Carragher BO, Cain SM, Pechatnikova E, Wilson-Kubalek EM, Whittaker M, et al. 1999. A structural change in the kinesin motor protein that drives motility. Nature 402(6763):778–784.

Saxton WM, Hicks J, Goldstein LS, Raff EC. 1991. Kinesin heavy chain is essential for viability and neuromuscular functions in *Drosophila*, but mutants show no defects in mitosis. Cell 64(6):1093–1102.

Stamer K, Vogel R, Thies E, Mandelkow E, Mandelkow EM. 2002. Tau blocks traffic of organelles, neurofilaments, and APP vesicles in neurons and enhances oxidative stress. J Cell Biol 156(6):1051–1063.

Stokin GB, Lillo C, Falzone TL, Brusch RG, Rockenstein E, Mount SL, Raman R, Davies P, Masliah E, Williams DS, et al., 2005. Axonopathy and transport deficits early in the pathogenesis of Alzheimer's disease. Science 307(5713):1282–1288.

Tanaka Y, Kanai Y, Okada Y, Nonaka S, Takeda S, Harada A, Hirokawa N. 1998. Targeted disruption of mouse conventional kinesin heavy chain, kif5B, results in abnormal perinuclear clustering of mitochondria. Cell 93(7):1147–1158.

Taute KM, Pampaloni F, Frey E, Florin E-L. 2008. Microtubule dynamics depart from the wormlike chain model. Phys Rev Lett 100(2):028102.

Thompson WC, Wilson L, Purich DL. 1981. Taxol induces microtubule assembly at low temperature. Cell Motil 1(4):445–454.

Trinczek B, Ebneth A, Mandelkow EM, Mandelkow E. 1999. Tau regulates the attachment/detachment but not the speed of motors in microtubule-dependent transport of single vesicles and organelles. J Cell Sci 112(Pt 14):2355–2367.

Valdman D, Atzberger Paul J, Yu D, Kuei S, Valentine Megan T. 2012. Spectral analysis methods for the robust measurement of the flexural rigidity of biopolymers. Biophys J 102(5):1144–1153.

Vershinin M, Carter BC, Razafsky DS, King SJ, Gross SP. 2007. Multiple-motor based transport and its regulation by Tau. Proc Natl Acad Sci USA 104(1):87–92.

Wolf S, Barton D, Kottschade L, Grothey A, Loprinzi C. 2008. Chemotherapy-induced peripheral neuropathy: prevention and treatment strategies. Eur J Cancer 44(11):1507–1515.

Yildiz A, Tomishige M, Gennerich A, Vale RD. 2008. Intramolecular strain coordinates kinesin stepping behavior along microtubules. Cell 134(6):1030–1041.